NUCLEAR MAGNETIC RESONANCE TRANSVERSE RELAXATION TIMES OF WATER PROTONS IN SKELETAL MUSCLE

CARLTON F. HAZLEWOOD, DONALD C. CHANG, BUFORD L. NICHOLS, *and* DONALD E. WOESSNER

From the Departments of Pediatrics and Physiology, Baylor College of Medicine, and Texas Childrens Hospital and Department of Physics, Rice University, Houston, Texas 77001, and Field Research Laboratory, Mobil Research and Development Corporation, Dallas, Texas 75221

ABSTRACT The observation of the spin-echo decay in a long time domain has revealed that there exist at least three different fractions of non- (or slowly) exchanging water in the rat gastrocnemius muscle. These fractions of water are characterized with different nuclear magnetic resonance (NMR) relaxation times and are identified with the different parts of tissue water. The water associated with the macromolecules was found to be approximately 8% of the total tissue water and not to exchange rapidly with the rest of the intracellular water. The transverse relaxation time (T_2) of the myoplasm is 45 ms which is roughly a 40-fold reduction from that of a dilute electrolyte solution. This fraction of water accounts for 82% of the tissue water. The reduced relaxation time is shown neither to be caused by fast exchange between the hydration and myoplasmic water nor by the diffusion of water across the local magnetic field gradients which arise from the heterogeneity in the sample. About 10% of the tissue water was resolved to be associated with the extracellular space, the relaxation time of which is approximately four times that of the myoplasm. Mathematical treatments of the proposed mechanisms which may be responsible for the reduction of tissue water relaxation times are given in this paper. The results of our study are consistent with the notion that the structure and/or motions of all or part of the cellular water are affected by the macromolecular interface and this causes a change in the NMR relaxation rates.

INTRODUCTION

Considerable studies on the properties of water in various physical systems have been reported in the past 10 years, which have led some investigators to propose that the interaction of water molecules with various surfaces results in the alteration of the physical properties of water. The notion that there are changes in the physical properties of water at various interfaces (surfaces) has been promoted by Drost-Hansen (1, 2). He has pointed out the importance of the mutual interactions between solvent and substrate, and that this interaction may occur over rather large distances. Furthermore, the work of Hori (3) reports that physical properties of water molecules may be altered by glass and quartz surfaces over distances as great as 1 or 2 μm.

Many of the techniques for studying water in physical systems, unfortunately, have not been applicable for study in biological systems. Nuclear magnetic resonance (NMR) spectroscopy, however, has been useful in the evaluation of the physical state of water in biological systems. The papers by Cope (4) and Hazlewood et al. (5) proposed that there exist no less than two phases[1] of ordered[2] water in many biological tissues including skeletal muscle. These workers proposed that one fraction of water is probably associated with the hydration of macromolecules and the other fraction was associated with water in both the cytoplasm and the extracellular space. Both of these fractions were characterized by relaxation times much shorter than those of pure water and were designated the minor and major phases of ordered water, respectively. Evidence from several non-NMR studies support the notion of at least two phases of tissue water (6–10).

The presence of exchange averaging was demonstrated for the major phase (5). Exchange between the major and minor phases could not be ruled out, but, if present, the exchange times were on the order of several hours (5). This interpretation has been reviewed by Damadian (11). Other investigators reported that only one relaxation time was observed for water in tissues (12–20).

The consistent obersvations[3] made for water protons in various tissues are, in comparison to pure water, a (*1*) reduction in the spin-lattice relaxation time (T_1) by a factor of four to five; (*2*) reduction of the spin-spin relaxation time (T_2) by a factor of about 50 (this is equivalent to the observed broadening of high resolution NMR signal); and (*3*) reduction in the diffusion coefficient by a factor of two (4, 5, 12–37). Several models were proposed to explain these observations.

(*a*) The shortened relaxation times reported for tissue water could result from paramagnetic impurities and/or by diffusion of water protons across local magnetic field gradients. These interpretations have been dealt with in numerous publications (4, 5, 15, 16, 27, 31, 33, 34, 37).

(*b*) The majority of the cellular water is free and in fast exchange with a small fraction of tightly bound water. This has been discussed in various publications (12, 14, 17–20, 33, 36) and will be a subject of discussion in this paper.

(*c*) The diffusion coefficient of cellular water may be reduced because of the compartmentalization of the tissue and the impedance of the actin-myosin filament system within the skeletal muscle (14–16). Experiments evaluating this proposed mechanism, however, led to the conclusion that neither were operative in skeletal muscle (24, 35, 38).

Rorschach et al. (38) predicted that there might be an anisotropy in the diffusion

---

[1]Here the word "phase" is used as originally intended, to be equivalent to fraction.

[2]The word "ordered" was used originally in reference 5. It was used to mean that the system behaves differently (in the NMR sense) in comparison to ordinary water. A reduction in molecular motion and/or a change in structure is suggested.

[3]Cope (4) and Hazlewood et al. (5) maintain that these findings are associated with the major fraction of tissue water. For a further discussion of this point, see reference 11 and the discussion in *Ann. N.Y. Acad. Sci.* (1973), **204**: 204–209.

coefficient of cellular water (that is, the diffusion of water in skeletal muscle in the radial direction would be less than in the longitudinal direction). This prediction was born out by experiment and once again the conclusion follows that the majority of the reduction of the diffusion coefficient cannot be accounted for by simple obstructive structures within the cell (35).

In November 1972 it was reported by Belton et al., that water protons in skeletal muscle could be described by three distinct transverse relaxation times (36). These observations confirm the existence of the minor phase water and indicate that the major phase water is comprised of, at least, two components. The findings of Belton et al. cast further doubt on the adequacy of the two-component fast-exchange model for cellular water. The present study was therefore instituted for two reasons: (*a*) to determine quantitatively, the multiple relaxation times in rat skeletal muscle and to determine the volume of water associated with each relaxation fraction; and (*b*) to evaluate the physical models that may or may not explain these findings.

METHODS

NMR Measurements

All NMR measurements were made on a spin-echo spectrometer in the Field Research Laboratory of Mobil Research and Development Corporation. The basic design of this spectrometer was described in references 39 and 40 and now has the additional feature of being digitally automated. The pulse intervals were obtained by countdown from a 1 MHz crystal oscillator. The spectrometer was operating at frequencies of 25 MHz and 50 MHz in this study. Both method A (90°–180°) and method B (90°–180°–180°–180°....) pulse sequences of Carr and Purcell (41) have been used. To observe the fast-relaxing component of the protons the free induction decay signal following the 90° pulse was also measured. The pulse-width of the 90° pulse is 2μs and active damping of pulse transients is employed. The "dead-time" of the system was observed to be about 10 μs by using pure water as the testing sample. The free induction decay signal reaches 99% of the full amplitude at 12 μs after the 90° pulse is turned on. The signal amplitude is always measured with a boxcar signal averager (42), the gatewidth of which can be set as small as 2 μs (in the case of free induction decay measurements). When the "boxcar" was used to measure the height of echoes, the gatewidth was set to be either 100 μs or 10 μs. The linearity of the detection system has been carefully calibrated. All data were corrected by computer against a standard calibration curve.

The temperature of the sample is maintained at room temperature (24°C) by flowing compressed air over the sample tube.

Sample Preparation

White rats obtained from the Texas Inbred Mouse Company were killed by cervical fracture and the gastrocnemius muscle was quickly removed from the body. The muscle was dissected free of fat and gross connective tissue and cut into pieces to insert into a 12 mm OD NMR tube. The sample was then centrifuged down to the bottom of the tube and placed in the spectrometer. A period of approximately 25 min was usually allowed before the first measurement was made to insure that the sample was at thermal equilibrium.

Determination of the Amount of Tissue Water

The wet weight of the tissue was measured with an electrical balance. The tissue was then put in an oven. After it was dried for approximately 12 h at 120°C, the dry sample was

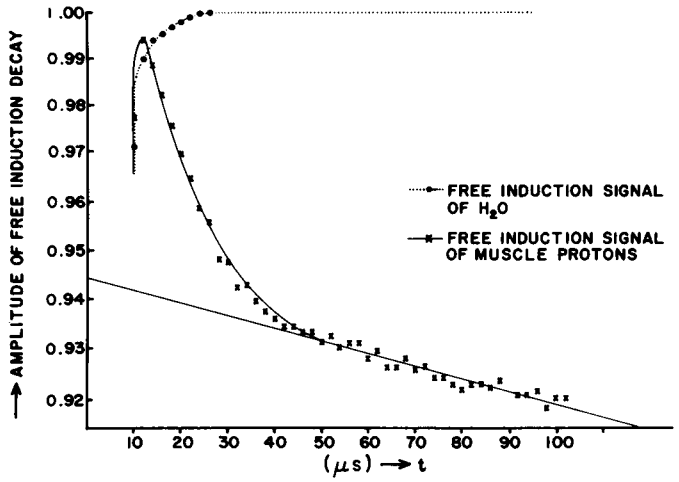

FIGURE 1 Free induction signal of proton after the 90° pulse. The gradual buildup of the pure water signal at small t shows the recovery of the receiver from the active-damping.

transferred into a vacuum chamber. It was pumped for 4 days at a vacuum about 0.05 torr and was continuously heated by an infrared light at an ambient temperature around 100°C. Finally, the heat source was removed and the sample was pumped for a few extra hours in higher vacuum. The dry weight was then determined.

RESULTS

Free Induction Decay

The shape of the free induction decay of the protons in muscle is neither exponential nor Gaussian. In Fig. 1, the initial amplitudes of the free induction decay are plotted vs. time in a semilog fashion. (The free induction decay of a pure water sample is also

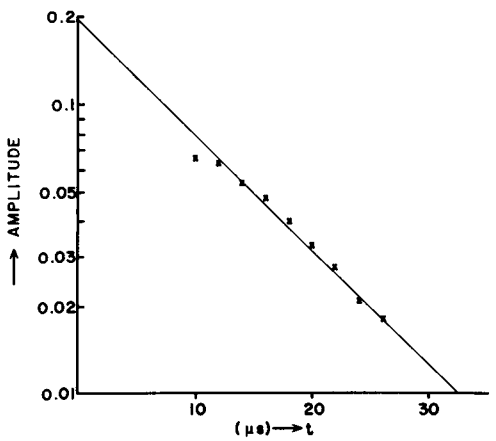

FIGURE 2 The free induction decay of the fast-relaxing fraction of muscle protons.

TABLE I

FAST-RELAXING FRACTION OF TISSUE PROTONS DETECTED IN THE FREE INDUCTION DECAY SIGNAL

T_2 is the transverse relaxation time which characterizes these protons. The relative population was estimated under the assumption that this fraction of protons follows simple exponential decay (see text).

Exp. no.	T_2	Intercept	Relative population in all protons
	μs		
06167208	16.7	0.197	0.165
07127204	16.4	0.180	0.153
07137204	15.4	0.198	0.165
07147205	15.2	0.237	0.192
Average	15.9	0.203	0.169
SD	±0.7	±0.024	±0.016

plotted for comparison.) The muscle proton signal decays rapidly first and then gradually levels off. This suggests that part of the protons in the muscle tissue undergoes fast relaxation. We separate this fast-relaxing fraction by subtracting the slowly varying component from the total free induction signal and then plotting this difference vs. time (See Fig. 2). This fast-relaxing component fits a single exponential curve and the transverse relaxation time is estimated to be very close to 16 μs. (The exact data are summarized in Table I.) Estimation of the population of these fast-relaxing protons is difficult because we do not know whether the simple exponential decay is also valid for the first 10 μs when the received signal is actively damped. If one makes the assumption that it is, then a population fraction of about 17% for the fast-relaxing protons can be inferred from the intercept of the ordinate.

90°–180° Measurements

Fig. 3 shows the amplitude of the echoes as a function of time (2τ). The echo amplitude has been normalized by taking the amplitude of the free induction signal at 100 μs after the 90°pulse as unity. From Fig. 3, it is apparent that the amplitude decay is not a simple exponential and thus the spin-spin relaxation rate cannot be described by one single T_2.

Diffusional Effect. The curvature in the echo amplitude plot cannot be attributed to the diffusional effect, since the diffusion would cause the decay curve to bend downward rather than upward from a straight-line fit. The diffusional decay in the normal operating condition is quite small in comparison to the T_2 relaxation; however, we monitored the echo signal at an observation time (2τ) as long as 600 ms, and the diffusional effect cannot be neglected. The spectrometer used in this study is equipped with a Varian 12-in high-resolution magnet which provides a reasonably

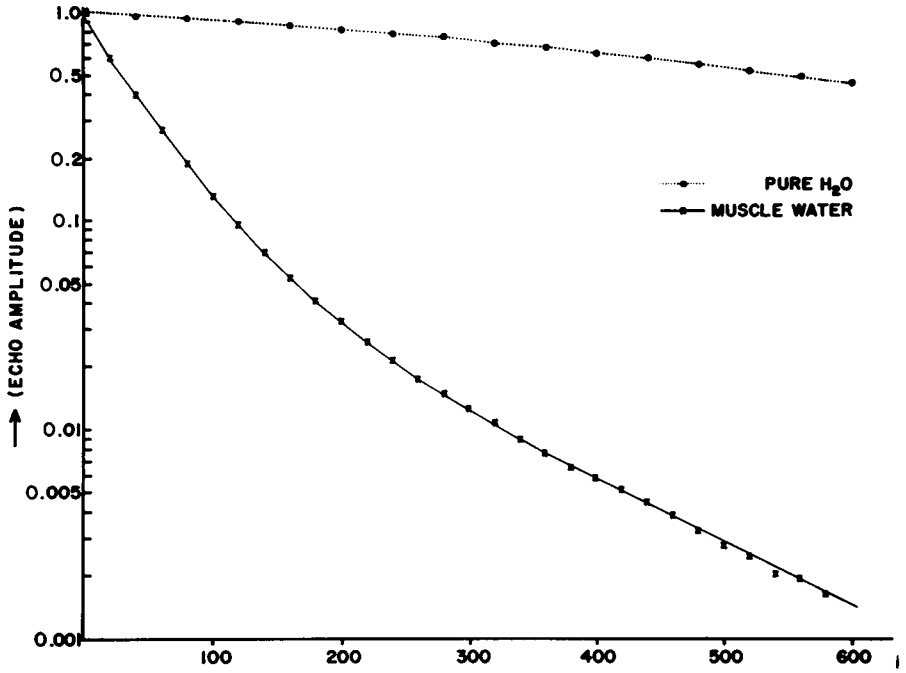

FIGURE 3 The echo decay as measured with the 90°-180° two-pulse method.

homogeneous field. (The free induction signal of pure water decays to half at about 10 ms.)

The diffusion coefficient (D) of muscle water at different 2τ was measured in order to estimate this diffusional decay. This was done with the conventional spin-echo method. Namely, D is calculated from the echo decay when a known magnetic field

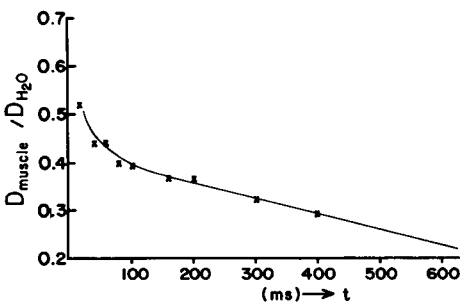

FIGURE 4

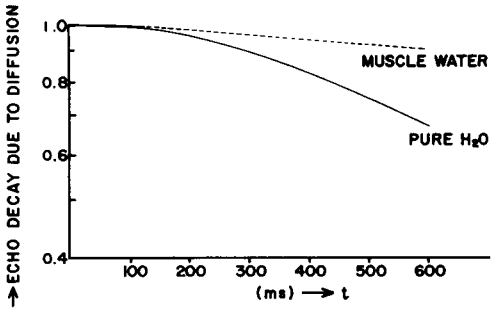

FIGURE 5

FIGURE 4 The change of diffusion coefficient of water protons as a function of the observation time (2τ). The diffusion coefficient was measured with a static field gradient spin-echo method.
FIGURE 5 The decay of echo amplitude due to diffusion alone. The "pure H_2O" curve was calculated from the data in Fig. 3. The "muscle water" curve was calculated from the "pure H_2O" curve and the data in Fig. 4 by the use of Eq. 1 in the text.

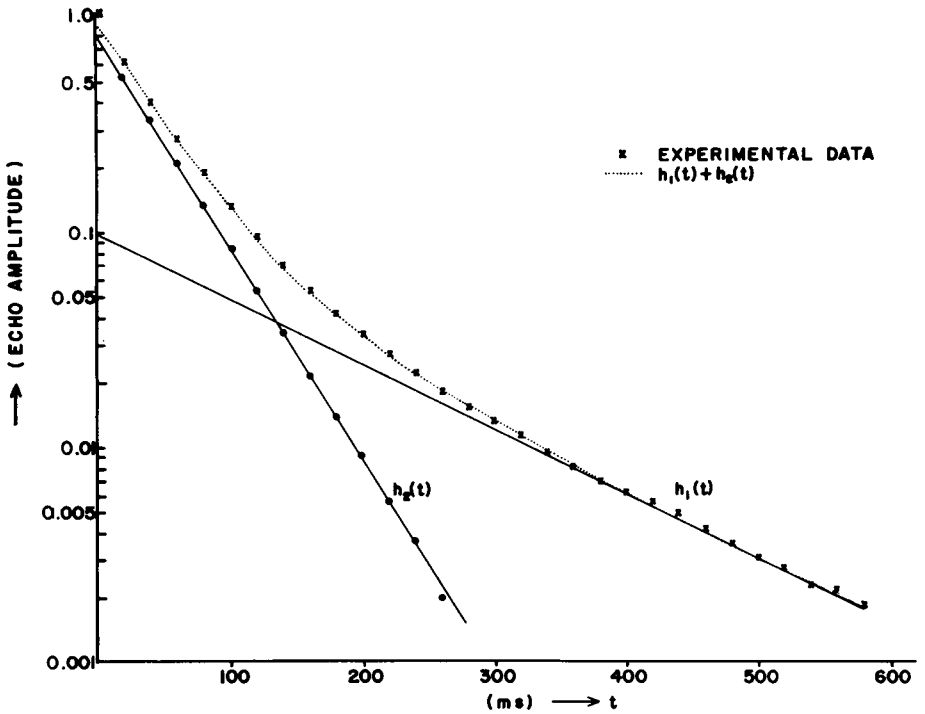

FIGURE 6 A Echo decay in a 90°–180° measurement on muscle. This figure is actually a replot of Fig. 3 after the data were corrected for diffusional decay. See text for the definition of $h_1(t)$ and $h_2(t)$.

gradient is applied. The measured diffusion coefficient is smaller than the diffusion coefficient of pure water. The ratio between the diffusion coefficient of muscle (D_{muscle}) and that of water (D_{H_2O}) is plotted in Fig. 4 as a function of the observation time (2τ). Theoretically, the diffusional contribution to the echo decay of muscle water is:

$$\exp\left\{-\frac{2}{3}\gamma^2 G^2 D_{\text{muscle}}\tau^3\right\} = \left[\exp\left\{-\frac{2}{3}\gamma^2 G^2 D_{H_2O}\tau^3\right\}\right]^{\xi}, \quad (1)$$

where γ is the gyromagnetic ratio, G is the static magnetic field gradient, and ξ equals $D_{\text{muscle}}/D_{H_2O}$. Within the braces in the right-hand side of the equation is the diffusional decay of a pure water sample, which can be easily measured and is shown in Fig. 5. Using the above equation, the diffusional contribution to the echo decay of muscle water at different 2τ can be calculated. The result is also shown in Fig. 5.

Curve Decomposition. After being corrected for the diffusional decay, the typical result of a 90°–180° measurement is shown in Fig. 6 A. It clearly indicates that there are multiple fractions of tissue water which involve distinct spin-spin relaxation

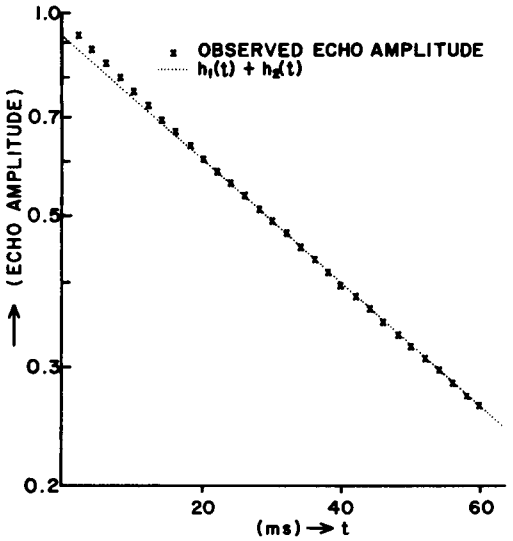

FIGURE 6 B Blowup of the first part of Fig. 6 A. Data which were measured in shorter time intervals were added.

times. One may assume that the measured signal is a summation of the signals from several non- (or slowly) exchanging fractions, i.e.,

$$h(t) = \sum_i h_i(t) \tag{2A}$$

and

$$h_i(t) = h_{oi} \exp\left\{-t/T_{2,i}\right\}, \tag{2B}$$

where $h(t)$ is the normalized echo amplitude at time ($t = 2\tau$), h_{oi} and $T_{2,i}$ are the relative population and the transverse relaxation time of the i^{th} fraction. This model does not exclude the possibility that within each $h_i(t)$ there may be several fast-exchanging subfractions. But those fractions which fast-exchange with each other will show a single T_2 and will appear to be as one fraction. What is important to know is the minimum number of (non- or slowly-exchanging) fractions needed to fit the observed data.

We start first by trying to fit the data with two fractions. We follow the usual procedures of curve decomposition by finding the slowest decaying fraction and subtracting this fraction from the observed data. As can be easily seen from Fig. 6 A, the observed $h(t)$ approaches a straight line when $t(t = 2\tau)$ is larger than 350 ms. This suggests that $h(t)$ is predominantly composed of the slowest relaxing fraction for $t > 350$ ms. The straight line which fits this part of the decay curve is then labeled $h_1(t)$. The points resulting from the subtraction of $h_1(t)$ from the decay curve can be fit with another straight line in the semilog plot (see Fig. 6 A). This straight-line fit

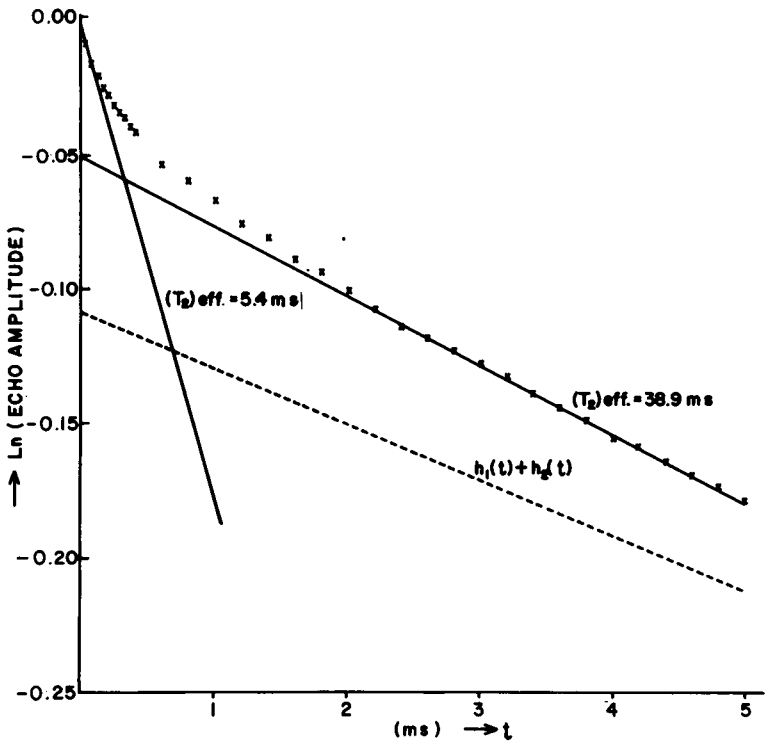

FIGURE 6 C The initial portion of the echo decay curve in a 90°-180° measurement on muscle. Echoes were measured in very small time intervals. The $h_1(t) + h_2(t)$ curve is the same as those in Fig. 6 A and Fig. 6 B.

is called $h_2(t)$. The sum $h_1(t) + h_2(t)$ closely approximates the observed $h(t)$, except when t is close to 0 (see Fig. 6 B). This indicates that there may be more than two fractions of non- (or slowly) exchanging tissue water. The initial part of the echo decay curve has been studied very carefully. There is a visible curvature change at t less than 1 ms (see Fig. 6 C). The initial rate of echo decay is 0.188 $(\text{ms})^{-1}$, which is equivalent to an effective relaxation time of 5.4 ms. This short relaxation time is evidence that a fast-relaxing fraction of muscle protons must exist. It can be easily shown that the initial slope of the echo decay curve in a multifraction spin system is given by

$$\sum_i \frac{h_{oi}}{T_{2,i}}.$$

Since the sum of h_{oi} is normalized to unity, the initial slope must be less than the reciprocal of the shortest T_2 value. The T_2^{-1} values of $h_1(t)$ and $h_2(t)$ in our study are 0.0063 and 0.023 $(\text{ms})^{-1}$, respectively. There must, therefore, be at least one additional fraction which involves a T_2 shorter than 5 ms.

In fact, if we assume that the muscle water can be decomposed into three non- (or

TABLE II

RESULTS OF THE 90°–180° MEASUREMENTS

P_1, P_2, and P_3 designate the population of the three fractions of tissue water. $T_{2,i}$ is the transverse relaxation time of the ith fraction. $T_{2,3}$ cannot be accurately determined because it is extremely sensitive to the way of fitting; however, it is estimated to be less than 5 ms (see Fig. 6 B).

Exp. no.	P_1	$T_{2,1}$	P_2	$T_{2,2}$	P_3
		ms		*ms*	
07127205	0.117	144.2	0.812	42.32	0.071
07137205	0.087	160.4	0.827	43.80	0.086
07147205	0.099	144.4	0.828	44.23	0.073
05077310	0.0895	170.5	0.851	44.51	0.060
Average	0.098	155	0.830	43.7	0.072
SD	±0.014	±13	±0.016	±1.0	±0.011

slowly) exchanging fractions, the spin-spin relaxation time of the third fraction can be calculated from the initial slope of the echo decay curve. Using the values of h_{oi} and $T_{2,i}$ listed in Table II, we find $T_{2,3}$ equal to 0.42 ms.

Carr-Purcell (90°–180°–180°–180° · · ·) Measurements

To confirm the 90°–180° data, we have performed a number of Carr-Purcell measurements with the Meiboon and Gill phase correction (43). The results appear to be very similar to those obtained from the two-pulse measurements. A typical Carr-Purcell spin-echo decay curve is shown in Fig. 7. Since the diffusional effect on a Carr-Purcell measurement is much smaller than that in the two-pulse measurements, there is no need to go through the procedure for diffusional correction. The data were analyzed in a similar manner as described in the preceding section. But since 2τ extends only to 300 ms, the echo decay has not reached its asymptote at the end of the measurement. We have to employ an iteration method to decompose the curve. The procedure follows: First we draw a tangential line to the data curve at t = 300 ms and designate it

$$h_1'(t) = \text{the first approximation of } h_1(t).$$

Then we subtract $h_1'(t)$ from the experimental data $h(t)$. The resultant data points are fit with a straight line which is called

$$h_2'(t) = \text{the first approximation of } h_2(t).$$

Subtracting $h_2'(t)$ from $h(t)$ for t from 200 ms to 300 ms, one can fit another tangential line and it is called

$$h_1''(t) = \text{the second approximation of } h_1(t).$$

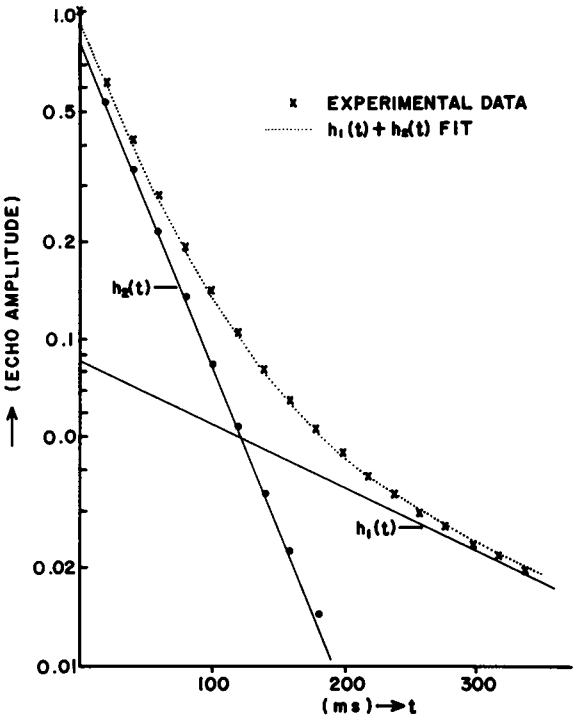

FIGURE 7 Echo decay in a Carr-Purcell measurement on muscle. The difference between the measured echo amplitude and $h_1(t)$ was shown by the circular data point.

Knowing the $h_1''(t)$, one can then find the second approximation of $h_2(t)$ [i.e., $h_2''(t)$] by peeling $h_1''(t)$ from the experimental data. Usually, the second approximation gives an almost perfect straight-line fit for all the data points except for the first data point. Further calculation following the same iteration procedures seems to improve (or change) the fitting very little. Therefore, the second approximation is used as the best fit. The results of a typical fit are shown in Fig. 7.

TABLE III
RESULTS OF CARR-PURCELL MEASUREMENTS
The definition of P_i and $T_{2,i}$ is the same as in Table II.

Exp. no.	P_1	$T_{2,1}$	P_2	$T_{2,2}$	P_3
		ms		*ms*	
07127207	0.093	147.7	0.830	44.45	0.077
05077312	0.108	216.4	0.843	44.75	0.079
05077315	0.113	194.7	0.808	45.67	0.079
05097308	0.086	223.4	0.827	43.73	0.087
Average	0.100	195.55	0.820	44.65	0.0805
SD	±0.0126	±34.16	±0.011	±0.803	±0.0044

TABLE IV

RELATIVE POPULATION OF TISSUE WATER PROTONS WHICH WERE DETECTED IN THE FREE INDUCTION SIGNAL AT $t = 100\,\mu s$

The first column gives the ratio of weight between the tissue water and a given pure water sample. The second column gives the ratio of the free induction signal amplitude between the tissue water and the pure water sample as measured at $t = 100\,\mu s$. The figure in this column has been corrected for the change of Q factor in the sample probe (see text). The figure in the last column was obtained by dividing the figure in the second column with figure in the first column.

Sample no.	Weight ratio $\left(\frac{\text{tissue water}}{\text{pure } H_2O}\right)$	Magnetization ratio $\left(\frac{\text{tissue water}}{\text{pure } H_2O}\right)$	Relative population of water protons detected at $t = 100\,\mu s$
1	1.0149	1.0365	1.0213
2	1.0355	1.0690	1.0324
3	1.1157	1.1093	0.9943
4	0.9913	0.9555	0.9636
5	0.9995	0.9133	0.9138
6	0.9649	0.9387	0.9728
Average			0.9831 ± 0.0431

The results of the Carr-Purcell measurements are tabulated in Table III. It is evident that at least three distinguishable fractions of water protons are needed to fit the complete echo decay curve. The population and relaxation time of each fraction is roughly the same as the value found in the two-pulse measurements.

In this study, we have also determined the amount of tissue water detected by the NMR spectrometer. The free induction signal at 100 μs following the 90° pulse was measured with a boxcar integrator. Muscle and pure water samples in a given volume were measured subsequently with identical spectrometer settings. The amplitude of the signal then gave the amount of NMR visible water in the sample. Because the Q factor of the sample coil is sensitive to the electrical conductivity of the sample, the sensitivity of the spectrometer is expected to change slightly when different samples are inserted into the probe. This has been calibrated by measuring a reference signal from a signal generator with different samples in the coil. The sensitivity of the spectrometer was found to be 1.7% smaller when the sample was changed from pure water to muscle. The data were corrected accordingly.

The actual amount of tissue water was determined by a vacuum drying procedure as described in the Methods section. The results are summarized in Table IV showing that approximately 98.3% of the tissue water was detected by the NMR spectrometer at 100 μs after the 90°pulse.

DISCUSSION

Identification of Relaxation Fractions

The fastest transverse relaxation time (T_2) recorded in this study is 16 μs and most likely comes from the protons on the macromolecules (membranes, proteins, and nu-

cleic acids) within the skeletal muscle samples. The multiple proton relaxation times seen in the two-pulse and in the Carr-Purcell measurements are protons of tissue water.

It should be noted that the T_2 values of these three fractions of water are much shorter than the T_2 of pure water or Ringer's solution ($T_2 \sim 1.6$ s). This reduction in T_2 is believed to result from the interaction between water and the macromolecules in the tissue. It is tempting to identify the slowest relaxing fraction [i.e., $h_1(t)$] as the extracellular fluid, since the concentration of macromolecules is minimum in the extracellular space. Our estimated population for this fraction is equivalent to 7.6% of the total muscle weight. A frequently quoted figure for extracellular space is 13%, obtained from an estimation of short-term inulin distribution by Boyle et al. (44). But a later study by Ling and Kromash using a new probe material, poly-L-glutamate, found the true extracellular space could not exceed 8% (45), which agrees very well with our figures.

The third fraction [i.e., $h_3(t)$] of tissue water (which is characterized by a much shorter relaxation time) can be easily identified with the hydration water molecules of the cellular proteins and other macromolecules. Both the translational and rotational motions of the hydration water molecules may be greatly hindered and therefore exhibit a much longer correlation time (which leads to a short T_2). The muscle contains about 20–25% dry solids. The population of $h_3(t)$ listed in Table II is 7.2%. This means that our measurements find approximately 0.3 g of hydration water per g of macromolecules, which agrees with the results of other studies (46).

The major portion of muscle water is contained inside the cell in the form of myoplasm, with which we identify the fraction $h_2(t)$. Since this fraction involves a medium relaxation rate and accounts for 82% of the total tissue water, some of the earlier studies which observed the echo decay in a small time domain would find the transverse magnetization of tissue water completely dominated by this fraction and thus appear to have a single relaxation rate. This second fraction of cellular water exhibits a 40-fold reduction of T_2 in comparison to pure water. As we mentioned in the Introduction, the cause of this reduction is a controversial matter. Nevertheless, the information we now have should enable us to evaluate some of the interpretations previously put forth. The observation of three water proton fractions requires that exchange between these three fractions be considered.

Effects of Exchange on Relaxation Times

The exchange can drastically alter the observed relaxation times, and our observation of multicomponent relaxation behavior allows us to discuss the T_2 behavior in more detail than could be done when only single-component behavior was apparent. In order to simplify the discussion, we will restrict our consideration to the general case of exchange of protons between two compartments. To relate the phenomenon of exchange to the biological problem at hand the compartments will be represented by hydration water and myoplasmic water. Judging from the excellent fit in Fig. 6 A, the myoplasmic water apparently can be regarded as existing in a uniform environment. The hydration water, as seen in Fig. 6 C, probably represents more than one fraction;

however, we regard it as a single component for simplicity. The details of this quantitative discussion of exchange is given as follows.

The nuclei are assumed to transfer between two different relaxation environments labeled by a, and b. Let T_a equal the longer relaxation time; P_a, population fraction of protons having T_a; τ_a, average residence time of a proton in a before it transfers to b; T_b, the shorter relaxation time; P_b, population fraction of protons having T_b; and τ_b, average residence time of a proton in b.

The constraints of the system include $P_a + P_b = 1$ and, by detailed balance, $P_a/\tau_a = P_b/\tau_b$. Also, T_a and T_b are assumed to be independent of τ_a and τ_b.

The proton transfer or exchange results in a transfer of nuclear spin magnetization between a and b. If the nuclear magnetization is changed from the equilibrium value, as by a pulse, the approach of the magnetization to the equilibrium value is governed by the differential equations

$$d(\Delta m_a)/dt = -(\Delta m_a/T_a) - (\Delta m_a/\tau_a) + (\Delta m_b/\tau_b), \tag{3}$$

$$d(\Delta m_b)/dt = -(\Delta m_b/T_b) - (\Delta m_b/\tau_b) + (\Delta m_a/\tau_a), \tag{4}$$

where Δm_a is the deviation from the equilibrium value for either transverse or longitudinal spin magnetization magnitude. The solution of these simultaneous equations gives the normalized relaxation curve:

$$h(t) = P'_a \exp(-t/T'_a) + P'_b \exp(-t/T'_b), \tag{5}$$

where

$$\begin{aligned} 1/T'_a &= C_1 - C_2, \\ 1/T'_b &= C_1 + C_2, \\ P'_b &= \frac{1}{2} - \frac{1}{4}\left[(P_b - P_a)\left(\frac{1}{T_a} - \frac{1}{T_b}\right) + \frac{1}{\tau_a} + \frac{1}{\tau_b}\right]/C_2, \\ P'_a &= 1 - P'_b, \end{aligned} \tag{6}$$

in which

$$C_1 = \frac{1}{2}\left[\frac{1}{T_a} + \frac{1}{T_b} + \frac{1}{\tau_a} + \frac{1}{\tau_b}\right] \tag{7}$$

$$C_2 = \frac{1}{2}\left[\left(\frac{1}{T_b} - \frac{1}{T_a} + \frac{1}{\tau_b} - \frac{1}{\tau_a}\right)^2 + \frac{4}{\tau_a \tau_b}\right]^{1/2}. \tag{8}$$

The parameters in Eq. 5 obey the general relationship

$$(P'_a/T'_a) + (P'_b/T'_b) = (P_a/T_a) + (P_b/T_b), \tag{9}$$

so that the initial slope is independent of the exchange rate.

In the limiting case τ_a and $\tau_b = \infty$, $P'_a = P_a$, $T'_a = T_a$, $P'_b = P_b$, and $T'_b = T_b$. In the opposite limiting case, $\tau_a, \tau_b \ll T_a, T_b$, the value of P'_b becomes vanishingly small and the relaxation curve becomes

$$h(t) = \left\{\exp -t\left(\frac{P_a}{T_a} + \frac{P_b}{T_b}\right)\right\}. \tag{10}$$

This is the fast exchange limit in which the observable relaxation rate is independent of the exchange rate and the multicomponent relaxation behavior is masked by the exchange.

In most of the earlier studies on tissue water, the relaxation curve was studied in a rather limited time domain and thus appeared to fit a single exponential decay. Some investigators then proposed that the observed relaxation rate is the result of a rapid exchange between the "bound" (hydration) water and the rest of intracellular water. This interpretation is not in agreement with the results of our study. As shown in Figs. 6 A–C, the difference between the relaxation rates of the myoplasmic water and the hydration water is clearly visible. The multicomponent behavior is not masked by the exchange. Hence, the intracellular water is not in the rapid exchange limiting case and the reduction in the observed T_2 cannot be explained by Eq. 10.

In the limit where τ_a and τ_b are infinite, the relaxation curve is the expected sum of the curves from the two relaxation environments a and b. With increasing exchange rate, the observable parameters deviate from those "inherent" to a and b. An interesting and pertinent case is when $T_a \gg T_b$. In this case, the observable population fractions are approximately P_a and P_b until $\tau_b/T_b \lesssim 1$. When τ_b becomes small enough so that $\tau_b/T_b \ll 1$, P'_b is nil and P'_a is unity. The observable T'_b does not change much from T_b until $\tau_b/T_b < 1$, then it decreases rapidly with further decrease of τ_b.

Hence, observable multicomponent behavior can be used to place limits on relaxation times and exchange rates among these components. If two-component behavior is observed, then one can establish approximate limiting values:

$$\begin{aligned} P'_a &\approx P_a \\ P'_b &\approx P_b \\ T'_b &\approx T_b \\ \tau_b &\gtrsim T_b \end{aligned} \tag{11}$$

However, in this case, T'_a can be much smaller than T_a. (Hence, the direct use of T'_a in determining correlation times can be invalid when this occurs.)

When $T_a \gg T_b$ and $P_a \gtrsim P_b$, a good approximation to T'_a can be obtained as follows. C_2 can be rewritten and substituted into Eq. 6, then,

$$\frac{1}{T'_a} = C_1\left\{1 - \left[1 - \frac{1}{C_1^2}\left(\frac{1}{T_a T_b} + \frac{1}{\tau_b T_a} + \frac{1}{\tau_a T_b}\right)\right]^{1/2}\right\}. \tag{12}$$

Recognizing that $1/T_a' \ll C_1$ under the above conditions, we see that the quantity in the square root brackets is close to unity. Then, using the approximation

$$[1 - x]^{1/2} \cong 1 - \tfrac{1}{2}x,$$

which is very good when x is small compared with unity, we obtain

$$\frac{1}{T_a'} \cong \frac{1}{2C_1}\left(\frac{1}{T_aT_b} + \frac{1}{\tau_bT_a} + \frac{1}{\tau_aT_b}\right). \tag{13}$$

Rewriting,

$$\frac{1}{T_a'} = \frac{1}{2C_1}\frac{1}{T_a}\left(\frac{1}{T_b} + \frac{1}{\tau_b}\right) + \frac{1}{2C_1}\frac{1}{\tau_aT_b}. \tag{14}$$

Then, under our condition $T_a \gg T_b$,

$$2C_1 \cong \frac{1}{T_b} + \frac{1}{\tau_a} + \frac{1}{\tau_b}. \tag{15}$$

Using Eq. 15 and the detailed balance condition $P_a/\tau_a = P_b/\tau_b$ in Eq. 14, we obtain

$$\frac{1}{T_a'} \cong \frac{P_a}{T_a}\left(\frac{\tau_b + T_b}{P_a\tau_b + T_b}\right) + \frac{P_b}{P_a\tau_b + T_b}. \tag{16}$$

(Note that this approximation reduces to Eq. 10 when τ_b is very small; also, $T_a' = T_a$ when $\tau_b \longrightarrow \infty$.)

A simpler approximation is obtained when $P_a/P_b \gg 1$. When this condition holds, Eq. 16 reduces to the further approximation

$$\frac{1}{T_a'} \cong \frac{1}{T_a} + \frac{P_b}{\tau_b + T_b}. \tag{17}$$

Eqs. 16 and 17 show in simple terms that the longer observable relaxation time depends on both the value of the shorter relaxation time and on the exchange rate. Using the approximate values in relation 11 when $T_a/T_a' \gg 1$ the limiting value of T_a' is:

$$T_a' \gtrsim 2T_b'/P_b'.$$

In our case, P_b' is the observable population of the hydration water (i.e., P_3) which is about 0.08. T_b' cannot be accurately determined because the hydration water may involve complex relaxation rates. Nevertheless, if we use the earlier estimated value of 0.42 ms, the limiting value for the transverse relaxation time of the myoplasmic water will be 12.8 ms which is not far from the value of 44 ms which we observed.

The exchange model with $\tau_b \approx T_b$ (we may call this case as "intermediate exchange") thus appears to be able to explain the reduction in the observable transverse relaxation time of the majority of cellular water. This model also is consistent with the observed variation of T_2 with temperature. According to Eq. 17, T_a' increases with both T_b and τ_b. The value of τ_b decreases with an increase in temperature, whereas T_b ordinarily increases with an increase in temperature. Hence, exchange will cause temperature independence of T_a' when the sum of T_b and τ_b is constant.

In determining whether the intermediate exchange case actually applies the most stringent test will be to determine the value of τ_b. This we cannot do directly yet. However, we can establish the limiting value of τ_b and compare it with other indirect measurements. According to relation 11, the lower bound of τ_b is approximately T_b' which may be put as 0.5 ms. From Eq. 17, the upper bound of τ_b can be estimated by assuming T_b is vanishingly small (i.e., $\tau_b < T_a' P_b$), which in our case gives about 3.6 ms. According to Hazlewood et al. (5), D_2O did not exchange with the minor phase muscle water (which is equivalent to our hydration water) in 24 h. This result strongly indicates that τ_b is much longer than the millisecond range and, therefore, the exchange rate is too slow and Eq. 17 is not applicable. Currently, we are planning to look deeper into the D_2O exchange experiments and hope to have a more direct estimate on the value of τ_b.

Relaxation Mechanisms

Our treatment of exchange is independent of the relaxation mechanisms responsible for the value of T_a and T_b, the relaxation times inherent to the relaxation environments. One relaxation mechanism which has been considered involves diffusion of water molecules across local magnetic field gradients, which arise because of the sample heterogeneity (15, 47). We have studied this mechanism following the approach of Klauder and Anderson (48). A simplified version of our study is given in the Appendix. We found that diffusion across the local field gradient cannot be the mechanism which results in the short value of T_2 for the cellular water.

The local field gradient arising from inhomogeneities in magnetic susceptibility in the sample should be proportional to the strength of the static magnetic field. If the diffusion across the local field gradient is primarily responsible for the shortening of the relaxation time, then T_2 should be inversely proportional to the square of the resonance frequency. We have determined T_2 of muscle water at 50 MHz (Fig. 8), and find that the relaxation time is practically unchanged in comparison with those studied at 25 MHz. We feel that the evidence is sufficient to reject this proposed mechanism.

Some investigators have suggested that relaxation of protons by paramagnetic impurities may be responsible for the observed shortening of the relaxation times of the tissue water. Since the strength of the dipole-dipole relaxation is in general inversely proportional to the sixth power of the distance between the two nuclei, only the protons within the first hydration sphere of a paramagnetic ion need to be considered. The contribution of paramagnetic ions to relaxation rates of these protons have been calculated by Solomon (49) and Bleombergen (50). According to their calculations, the

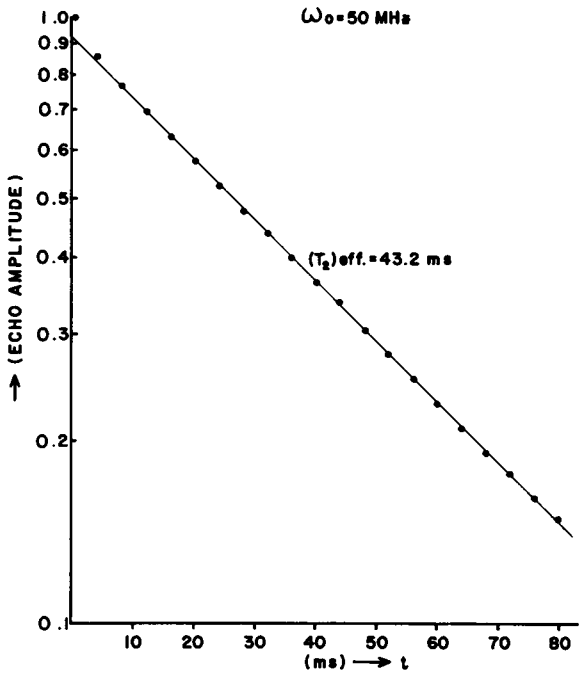

FIGURE 8 Echo decay of a 90°-180° measurement on muscle at a resonance frequency of 50 MHz. (All data reported from Figs. 1-7 were obtained at 25 MHz.)

inverse of $T_{1,2M}$ (relaxation times due to paramagnetic impurities) is proportional to γ_I^2 (γ_I is the gyromagnetic ratio of the nucleus). The dipole-dipole contribution is directly proportional to γ_I^2. The hyperfine structure coupling constant A is proportional to γ_I (51) and thus the scalar contribution is also directly proportional to γ_I^2. Since γ_I^2 for proton is 42.4 times larger than that for deuteron, the deuteron T_2 would be much longer than the proton T_2 if the paramagnetic effect is responsible for the short T_2 of protons. However, in comparing the data of Cope (4) with ours, the deuteron T_2 of muscle water is nearly an order-of-magnitude shorter than the proton T_2. Hence the effect of paramagnetic impurities on the relaxation times of muscle water is insignificant.

Other possible relaxation mechanisms include the magnetic dipole-dipole interactions between (*a*) the two protons in the same water molecules, (*b*) protons in different water molecules, and (*c*) protons of water molecules and nonexchangeable protons of macromolecules. However, the deuteron experiments of Cope (4) show that (*c*) is not of major importance. Also, the O^{17} experiments of Swift and Barr (34) also show that exchange of water and hydroxyl protons of macromolecules is of minor significance.

Hence, the significant mechanisms for the T_2 reduction are either (*a*) or (*b*), or both. The longitudinal and transverse relaxation of protons are governed by the directions, magnitudes and time dependences of the magnetic fields experienced by these protons.

Within each fraction of tissue water, the relaxation contributions from the magnetic dipole-dipole interactions between protons are given by the following equations (52):

$$\frac{1}{T_1} = G\sum_i P_i\left(\frac{\tau_{ci}}{1 + \omega_o^2\tau_{ci}^2} + \frac{4\tau_{ci}}{1 + 4\omega_o^2\tau_{ci}^2}\right), \tag{18}$$

$$\frac{1}{T_2} = \frac{1}{2}G\sum_i P_i\left(3\tau_{ci} + \frac{5\tau_{ci}}{1 + \omega_o^2\tau_{ci}^2} + \frac{2\tau_{ci}}{1 + 4\omega_o^2\tau_{ci}^2}\right), \tag{19}$$

where $\Sigma_i P_i = 1$, the τ_{ci} are various correlation times, G is an interaction constant, and ω_o is the NMR frequency. The dipole-dipole interactions depend on the distances between the protons in a pair, the orientation of the proton pair in the magnetic field H_o of the NMR spectrometer, and on the time dependences of these quantities. These quantities depend on the molecular structure and motions. The effects of the dipole-dipole interactions on the longitudinal and transverse relaxation times T_1 and T_2 can be obtained from the autocorrelation functions $[F(t)\ F^*(t + t')]_{av}$, in which F is a function of the length and orientation of the line drawn between the protons in a pair (49, 53). Ordinarily, the autocorrelation functions have the mathematical form

$$\langle F(t)F^*(t + t')\rangle_{av} = \langle F(t)F^*(t)\rangle_{av}\sum_i P_i \exp(-t'/\tau_{ci}), \tag{20}$$

so that the τ_{ci} in Eqs. 18 and 19 depend on the rates of the molecular motions. The various types of molecular motions can result in multiple correlation times. For example, anisotropic rotational motions of liquid molecules can contribute to the multiplicity. Eqs. 18 and 19 show that T_1 and T_2 are equal when the frequencies of molecular motions are much greater than the NMR frequency (i.e., when $\omega_o^2\tau_c \ll 1$).

The observed relaxation times of water in tissue are less than those of bulk water, and also $T_1 \gg T_2$. In order to interpret these observations, we need to take into account the complex environment of the water. Part of the water can be on specific adsorption sites on the macromolecules, part can be at the macromolecule-water interface, and part can be outside of these sites and interfacial regions. Our experimental results indicate that the adsorbed (hydration) water molecules do not exchange with the cytoplasmic water in a significant manner. But it is likely that the interfacial water and the rest of the cellular water will exchange. If exchange among the various environments does occur, the observable relaxation times will depend on the motions of the molecules in the various environments and on the exchange among these environments.

It is generally accepted that the observed relaxation phenomena result from interactions of the solid material with the water and possibly from modifications of water-water interactions. According to Frank and Wen (54), the existence of the solid surface will protect the water structure and reduce the motion of the water molecules. The presence of adsorption sites and the solid surface can have several effects. First, we might expect that the motions of these adsorbed and interfacial water molecules

are different from those of pure water. Second, the molecular orientations can be affected because the bonding and electrical charge distribution of the water molecule are nonspherical. Hence, the adsorbed and interfacial water molecules are likely to have both reduced and anisotropic motions and also have preferential orientations with respect to the solid material.

The preferential orientation, when it occurs, causes the autocorrelation function to depend on the arrangements of the adsorption sites and of the interfaces. This introduces a new *correlation time* which is a measure of the time required for a molecule to experience a random time-averaged orientation. If the neighboring sites and interfaces are randomly oriented, the τ_{ci} value can be sufficiently short so that T_1 and T_2 are equal. On the other hand, when these sites and interfaces are ordered over a sufficiently long range, a τ_{ci} can be sufficiently long so that $\omega_o\tau_{ci} > 1$ and cause $T_1 \gg T_2$. The NMR spectrum can be a doublet when the ordering is very long-range and when the average lifetime of a proton in a given water molecule is sufficiently long (intermolecular proton exchange has the effect of shortening the correlation time) (55, 56). Doublet spectra have been observed for water in contact with a number of organic and inorganic substrates (57–73), and preferential orientation may be one possible mechanism contributing to the shortening of the observed relaxation time.

At this point, it is clear that the observed relaxation properties of tissue water are caused by adsorption and the interfacial effect(s). An important question, however, remains unanswered. Namely, what portion of the cellular water is significantly influenced (in the sense of structure and property) by the macromolecular interface?

There are extremely different views on this question. Ling and Negendank (6), using the results of a muscle water vapor-equilibration study, reported that 95% of the muscle water is made up with polarized multilayers. (The remaining 5% is tightly adsorbed in the macromolecules.) Investigators who favor the two-fraction fast exchange model, on the other hand, generally assumed that the majority cellular water is no different from pure water. However, evidence from other studies in surface science appears to suggest that the interfacial water is significantly thick. A 1 μm thick film trapped between two glass plates (or quartz plates) was shown not to freeze at a temperature of −96°C (3). As the film thickness was reduced to 80 nm, the water vapor pressure dropped to below 0.01 mm Hg, even with temperature as high as 100°C (3). The dielectric constant of a 1 μm thick water thin film trapped between mica plates was also found to be one order of magnitude smaller than that of bulk water (74). It is reported in a study of water molecules in the polysaccharide B-1459 system that the size of the domains of non-randomly arranged macromolecules, in which the water molecules are preferentially oriented, can be as large as 15 μm (71). Since the average distance between a water molecule and the protein filaments in muscle is in the order of 10 nm, most of the cellular water is probably influenced by the macromolecular interface.

Before the completion of our work a paper by Belton et al. appeared which also reported the existence of three fractions of water in frog muscle (36). The quantities

they estimated in each fraction are consistent with ours except for the fastest relaxing fraction. This minor disagreement is probably due to the fact that different biological models were studied, and that different methods were used to choose the best fit. Their estimate of the population of the fastest relaxing fraction of water is about 20%. This is equivalent to 0.8 g of hydration water per g of dry solid, which is higher than the usually estimated figures obtained from the freezing studies on protein solutions (46, 75). Nevertheless, it is consistent with the results of their own freezing experiments in which approximately 20% of the tissue water was found unfrozen at temperatures below $-10°C$.

CONCLUSIONS

(*a*) From the results of the 90°–180° and Carr-Purcell measurements, it was found that there are at least three different fractions of non- (or slowly) exchanging water existing in the rat gastrocnemius muscle.

(*b*) The hydration water, which was found to be approximately 0.3 gram per gram of macromolecules, does not exchange rapidly with the rest of the intracellular water. This is inconsistent with the expectation from some earlier two-fraction fast-exchange models.

(*c*) The transverse relaxation time (T_2) of the myoplasm is 44 ms which is roughly a 40-fold reduction from that of a dilute electrolyte solution. This reduction was shown not to be caused by the diffusion of water molecules across the local magnetic field gradients which arise from the heterogeneity in the sample.

(*d*) The results of our study are consistent with the notion that the structure and/or motions of all or part of the cellular water is affected by the macromolecular interface and this causes a change in the NMR relaxation rates.

APPENDIX

Suppose that there is a Gaussian distribution of magnetic fields so that there is a Gaussian distribution of resonance frequencies ω. If the ω values are distributed along the diffusional path of the water molecules so that the covariance function

$$\langle \Delta\omega(t)\Delta\omega(o)\rangle = \langle \Delta\omega(o)^2\rangle \exp(-t/\tau_c) \tag{21}$$

is obeyed, where $\Delta\omega$ is the deviation from the average value, then the shape of the free induction decay following a 90° pulse is

$$h(t) = \exp\{-\sigma^2\tau_c^2[\exp(-t/\tau_c) + t/\tau_c - 1]\}. \tag{22}$$

For 90°–180° pulse sequences with the 180° pulse at time $t = \tau$,

$$h(2\tau) = \exp\{-\sigma^2\tau_c^2[2\tau/\tau_c - 3 - \exp(-2\tau/\tau_c) + 4\exp(-\tau/\tau_c)]\}. \tag{23}$$

TABLE V

VALUES OF $\sigma T_2^{\ddagger}$ AND $\sigma T_2\dagger$ COMPUTED FOR VARIOUS VALUES OF $\sigma\tau_c$ FOR A GAUSSIAN DISTRIBUTION OF ω VALUES

σ is the dispersion of the Gaussian distribution and τ_c is the correlation time which describes the time-dependence of the ω values experienced by a water molecule. $T_2^{\ddagger}$ and $T_2\dagger$ were defined in the text.

$\sigma\tau_c$	$\sigma T_2^{\ddagger}$	$\sigma T_2\dagger$
100.00	1.4176	10.770
56.234	1.4202	8.9461
31.623	1.4248	7.4540
17.783	1.4332	6.2393
10.000	1.4483	5.2593
5.6234	1.4761	4.4817
3.1623	1.5280	3.8855
1.7783	1.6292	3.4664
1.0000	1.8414	3.2517
0.56234	2.3317	3.3526
0.31623	3.4785	4.1090
0.17783	5.8012	6.1568
0.10000	10.100	10.300
0.056234	17.839	17.952
0.031623	31.654	31.717
0.017783	56.251	56.287

In these equations, σ is the root mean square value of $\Delta\omega$. These curves can be readily computed and the values of t and 2τ at which the respective curves have decayed to $1/e$ of their initial values can be obtained. These times are called T_2^* and $T_2\dagger$, respectively. When $\sigma\tau_c \gtrsim 1$, $T_2\dagger$ is greater than T_2^*. If H_o is sufficiently homogeneous, the observed value of T_2^* from the free induction decay following a 90° pulse is accurate. If T_2^* is less than $T_2\dagger$, then σ and τ_c can be evaluated by comparing these observed values with the theoretical values (see Table V). If the observed T_2^* value is equal to $T_2\dagger$, the value of $\sigma\tau_c$ is less than 0.1.

When $\sigma\tau_c < 0.1$, both curves are simple exponential decays with $1/T_2^* = 1/T_2\dagger = \sigma^2\tau_c$. Also, T_2 values from 90°–180° sequences will be the same as from Carr-Purcell sequences unless the Carr-Purcell pulse interval is near τ_c, in which case the Carr-Purcell value will be the larger one.

When $\sigma\tau_c > 10$, $T_2\dagger > T_2^{\ddagger}$, and the 90°–180° curve has the exponential t^3 decay. For intermediate values of $\sigma\tau_c$, the effective exponent on time is intermediate between 1 and 3.

If σ results from magnetic susceptibility effects, Eqs. 22 and 23 indicate that the argument in the exponential is directly proportional to H_o^2. The magnetic field independence of the observed T_2 then rules out this relaxation mechanism as being the cause of the short T_2 of the major fraction of the cellular water.

The assistance of Mrs. Mary Comerford in preparing this manuscript is acknowledged.

This work was supported by grants from The Robert A. Welch Foundation, The Liberty Muscular Dystrophy Research Foundation, and U.S. Public Health Service Research Grants GM-20154 and RR-0188 from the General Clinical Research Centers Program of the Division of Research Resources, National Institutes of Health, Bethesda, Md.

Received for publication 7 November 1973 and in revised form 13 February 1974.

REFERENCES

1. DROST-HANSEN, W. 1969. *Ind. Eng. Chem.* **61**:10.
2. DROST-HANSEN, W. 1971. Chemistry of the Cell Interface, Part B. H. D. Brown, editor. Academic Press, Inc., New York.
3. HORI, T. 1956. *Low Temp. Sci. Ser. A.* **15**:34.
4. COPE, F. W. 1969. *Biophys. J.* **9**:303.
5. HAZLEWOOD, C. F., B. L. NICHOLS, and N. F. CHAMBERLAIN. 1969. *Nature (Lond.).* **222**:747.
6. LING, G. N., and W. NEGENDANK. 1970. *Physiol. Chem. Phys.* **2**:15.
7. POCSIK, S. 1967. *Acta Biochim. Biophys. Acad. Sci. Hung.* **2**:149.
8. POCSIK, S. 1969. *Acta Biochim. Biophys. Acad. Sci. Hung.* **4**:395.
9. MCLAUGHLIN, S. G. A., and J. A. M. HINKE. 1966. *Can. J. Physiol. Pharmacol.* **44**:837.
10. MACOVSCHI, E. 1969. Biosctuctura. Acad. Repub. Social. Romania, Bucuresti.
11. DAMADIAN, R. 1973. CRC Critical Reviews in Microbiology. Chemical Rubber Company, Cleveland, Ohio.
12. BRATTON, C. B., A. L. HOPKINS, and J. W. WEINBERG. 1965. *Science (Wash. D.C.).* **147**:738.
13. FRITZ, O. G., and T. J. SWIFT. 1967. *Biophys. J.* **7**:675.
14. ABETSEDARAKAYA, L. A., F. G. MIFTAKHUTDINOVA, and V. D. FEDOTOV. 1968. *Biophysics (Engl. Transl. Biofiz.).* **13**:750.
15. HANSEN, J. R. 1971. *Biochim. Biophys. Acta.* **230**:482.
16. FINCH, E. D., J. F. HARMON, and B. H. MULLER. 1971. *Arch. Biochem. Biophys.* **147**:299.
17. COOKE, R., and R. WIEN. 1971. *Biophys. J.* **11**:1002.
18. COOKE, R., and R. WIEN. 1973. *Ann. N. Y. Acad. Sci.* **204**:197.
19. WALTER, J. A., and A. B. HOPE. 1971. *Prog. Biophys. Mol. Biol.* **23**:1.
20. WALTER, J. A., and A. B. HOPE. 1971. *Aust. J. Biol. Sci.* **24**:497.
21. ODEBLAD, E., B. N. BHAR, and G. LINDSTROM. 1956. *Arch. Biochem. Biophys.* **63**:221.
22. SWIFT, T. J., and O. G. FRITZ. 1969. *Biophys. J.* **9**:54.
23. HAZLEWOOD, C. F., B. L. NICHOLS, D. C. CHANG, and B. BROWN. 1971. *Johns Hopkins Med. J.* **128**: 117.
24. CHANG, D. C., H. E. RORSCHACH, B. L. NICHOLS, and C. F. HAZLEWOOD. 1973. *Ann. N. Y. Acad. Sci.* **204**:434.
25. DAMADIAN, R., M. GOLDSMITH, and K. S. ZANER. 1971. *Biophys. J.* **11**:761.
26. HAZLEWOOD, C. F., D. C. CHANG, B. L. NICHOLS, and H. E. RORSCHACH. 1971. *J. Mol. Cell. Cardiol.* **2**:51.
27. CHANG, D. C., C. F. HAZLEWOOD, B. L. NICHOLS, and H. E. RORSCHACH. 1972. *Nature (Lond.).* **235**: 170.
28. MOSORA, F. 1972. *Rev. Roum. Biochim.* **9**:51.
29. MILD, K. H., T. L. JAMES, and K. T. GILLEN. 1972. *J. Cell. Physiol.* **89**:155.
30. JAMES, T. L., and K. T. GILLEN. 1972. *Biochim. Biophys. Acta.* **286**:10.
31. CIVAN, M. M., and M. SHPORER. 1972. *Biophys. J.* **12**:404.
32. VICK, R. L., D. C. CHANG, B. L. NICHOLS, C. F. HAZLEWOOD, and M. C. HARVEY. 1973. *Ann. N. Y. Acad. Sci.* **204**:575.
33. OUTHRED, R. K., and E. P. GEORGE. 1973. *Biophys. J.* **13**:97.
34. SWIFT, T. J., and E. M. BARR. 1973. *Ann. N. Y. Acad. Sci.* **204**:191.
35. CLEVELAND, G. G., D. C. CHANG, H. E. RORSCHACH, D. E. WOESSNER, and C. F. HAZLEWOOD. 1973. *Fed. Proc.* **32**:302.
36. BELTON, P. S., R. R. JACKSON, and K. J. PACKER. 1972. *Biochim. Biophys. Acta.* **286**:16.

37. HOLLIS, D. P., J. S. ECONOMOU, L. C. PARKS, J. C. EGGLESTON, L. A. SARYAN, and J. L. CZEISLER. 1973. *Cancer Res.* **33**:2156.
38. RORSCHACH, H. E., D. C. CHANG, C. F. HAZLEWOOD, and B. L. NICHOLS. 1973. *Ann. N. Y. Acad. Sci.* **204**:444.
39. BUCHTA, J. C., H. S. GUTOWSKY, and D. E. WOESSNER. 1958. *Rev. Sci. Instrum.* **29**:55.
40. MCKAY, R. A. and D. E. WOESSNER. 1966. *J. Sci. Instrum.* **43**:838.
41. CARR, H. Y., and E. M. PURCELL. 1954. *Phys. Rev.* **94**:630.
42. CLARK, W. G., and A. L. KERLIN. 1967. *Rev. Sci. Instrum.* **38**:1593.
43. MEIBOOM, S., and D. GILL. 1958. *Rev. Sci. Instrum.* **29**:688.
44. BOYLE, P. J., E. J. CONWAY, F. KANE, and H. L. O'REILLY. 1941. *J. Physiol.* **99**:401.
45. LING, G. N., and M. H. KROMASH. 1967. *J. Gen. Physiol.* **50**:677.
46. KUNTZ, I. D., JR., T. S. BRASSFIELD, G. D. LAW, and G. V. PURCELL. 1969. *Science (Wash. D.C.).* **163**: 1329.
47. HANSEN, J. R., and K. D. LAWSON. 1970. *Nature (Lond.).* **225**:542.
48. Klauder, J. R., and P. W. ANDERSON. 1962. *Phys. Rev.* **125**:912.
49. SOLOMON, I. 1955. *Phys. Rev.* **99**:559.
50. BLOEMBERGEN, N. 1957. *J. Chem. Phys.* **27**:572.
51. LAUKIEN, G., and F. NOACK. 1960. *Z. Physik.* **159**:311.
52. WOESSNER, D. E. 1962. *J. Chem. Phys.* **37**:647.
53. BLOEMBERGEN, N., E. M. PURCELL, and R. V. POUND. 1948. *Phys. Rev.* **73**:679.
54. FRANK, H. S., and W. Y. WEN. 1957. *Discuss. Faraday Soc.* **24**:133.
55. WOESSNER, D. E., B. S. SNOWDEN, JR., and G. H. MEYER. 1969. *J. Chem. Phys.* **51**:2968.
56. WOESSNER, D. E., B. S. SNOWDEN, JR., and G. H. MEYER. 1970. *J. Colloid Interface Sci.* **34**:43.
57. DUCROS, P. 1960. *Bull. Soc. Fr. Mineral. Cristallogr.* **83**:85.
58. HECHT, A. M., M. DUPONT, and P. DUCROS. 1966. *Bull. Soc. Fr. Mineral. Cristallogr.* **89**:6.
59. WOESSNER, D. E., and B. S. SNOWDEN, JR. 1969. *J. Colloid Interface Sci.* **30**:54.
60. WOESSNER, D. E., and B. S. SNOWDEN, JR. 1969. *J. Chem. Phys.* **50**:1516.
61. HECHT, A. M., and E. GEISSLER. 1970. *J. Colloid Interface Sci.* **34**:32.
62. BREKHUNETS, A. G., V. V. MANK, F. D. OVCHARENKO, Z. E. SUYUNOVA, and YU. I. TRARASEVICH. 1970. *Teor. Eksp. Khim.* **6**:523.
63. BERENDSEN, H. J. C. 1962. *J. Chem. Phys.* **36**:3297.
64. MIGCHELSEN, C., and H. J. C. BERENDSEN. 1967. Magnetic Resonance and Relaxation. North-Holland Publishing Co., Amsterdam. 761.
65. DEHL, R. E., and C. A. J. HOEVE. 1969. *J. Chem. Phys.* **50**:3245.
66. CHARVOLIN, J., and P. RIGNY. 1969. *C. R. Acad. Sci. (Paris).* **B269**:224.
67. BLINC, R., K. EASWARAN, J. PIRS, M. VOLFAN, and I. ZUPANCIC. 1970. *Phys. Rev. Lett.* **25**:1327.
68. MIGCHELSEN, C., H. J. C. BERENDSEN, and A. RUPPRECHT. 1968. *J. Mol. Biol.* **37**:235.
69. LYNCH, L. J., and A. R. HALY. 1970. *Kolloid-Z.* **239**:581.
70. DEHL, R. E. 1968. *J. Chem. Phys.* **48**:831.
71. WOESSNER, D. E., and B. S. SNOWDEN, JR. 1973. *Ann. N. Y. Acad. Sci.* **204**:113.
72. LAWSON, K. D., and T. J. FLAUTT. 1967. *J. Am. Chem. Soc.* **89**:5489.
73. JOHANSSON, A., and T. DRAKENBERG. 1971. *Mol. Cryst. Liquid Cryst.* **14**:23.
74. PALMER, L. S., A. CUNLIFFE, and J. M. HOUGH. 1952. *Nature (Lond.).* **170**:796.
75. DEHL, R. E. 1970. *Science (Wash. D.C.).* **170**:738.